Gazi Üniversitesi
Fen Bilimleri Dergisi
PART C: TASARIM VE TEKNOLOJİ

Gazi University
Journal of Science
PART C: DESIGN AND TECHNOLOGY

GU J Sci, Part C, 12(4): 1145-1154 (2024)

Experimental Investigations of Sigma Vectors in Nodal Aberration Theory for Coma-Free Pivot Misalignment State of a Cassegrain Telescope

Meltem YEŞİLTEPE[1], Sefer Bora LİŞESİVDİN[2*]

[1]*Gazi University, Graduate School of Natural and Applied Science, Department of Advanced Technologies, 06560, Ankara, Türkiye*

[2]*Gazi University, Faculty of Science, Department of Physics, 06560, Ankara, Türkiye*

Article Info

Research article
Received: 18/11/2024
Revision: 02/12/2024
Accepted: 03/12/2024

Keywords

Nodal aberration theory
Coma-free pivot point (CFPP)
Cassegrain telescope Sigma vectors
Optical alignment

Makale Bilgisi

Araştırma makalesi
Başvuru: 18/11/2024
Düzeltme: 02/12/2024
Kabul: 03/12/2024

Anahtar Kelimeler

Nodal aberasyon teorisi
Koma-serbest dönme noktası (KSDN)
Cassegrain teleskop
Sigma vektörleri
Optik hizalama

Graphical/Tabular Abstract (Grafik Özet)

The study investigates the sigma vectors in Nodal Aberration Theory (NAT) for a Cassgerain telescope under CFPP misalignment. /Çalışma, CFPP hizalama kaçıklığı durumu altında bir Cassegrain teleskop için Nodal Aberasyon Teorisi'ndeki (NAT) sigma vektörlerini incelemektedir.

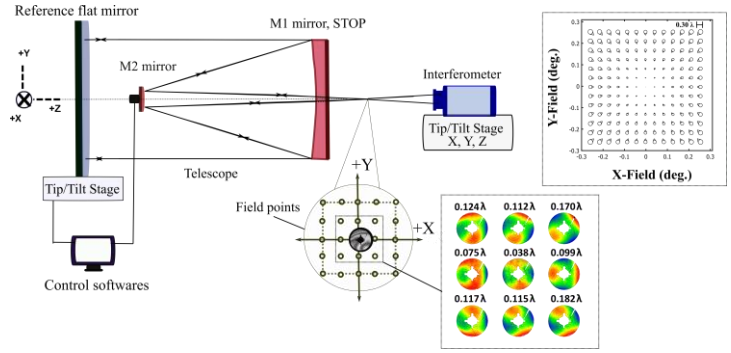

Figure A: *Experimental investihgations of sigma vectors on a Cassegrain telescope exhibiting CFPP misalignment/* ***Şekil A:*** *CFPP hizalama kaçıklığı sergileyen bir Cassegrain teleskop üzerinde sigma vektörlerin deneysel olarak araştırılması*

Highlights (Önemli noktalar)

- *The study presents an aberration analysis of a Cassegrain telescope./ Çalışma, Cassegrain teleskop için bir aberasyon analizi sunmaktadır.*
- *The study presents the experimental calculation of the field aberration vectors and sigma vectors for a Cassegrain telescope under CFPP misalignment./ Çalışma, CFPP hizalama kaçıklığı altındaki bir Cassegrain teleskop için alan aberasyon vektörlerinin ve sigma vektörlerinin deneysel hesaplamalarını sunmaktadır.*
- *The study presents the calculation of the misalignments of the telescope's secondary mirror and the corresponding Full Field Displays./ Çalışma, teleskobun ikinci aynasındaki hizalama kaçıklıklarını ve bu kaçıklıklar için tam alan görüntülerini hesaplamaktadır..*

Aim (Amaç): *This study analyzes the aberration state of a Cassegrain telescope under CFPP misalignment and experimentally calculates the sigma vectors./ Bu çalışma, CFPP hizalama kaçıklığında Cassegrain teleskobunun aberasyon durumunu analiz eder ve sigma vektörlerini deneysel olarak hesaplar.*

Originality (Özgünlük): *The originality of this study lies in its approach to experimentally calculating the sigma vectors for a Cassegrain telescope under CFPP misalignment./ Bu çalışmanın özgünlüğü, CFPP hizalama kaçıklığı altında Cassegrain teleskobu için sigma vektörlerini deneysel olarak hesaplama yaklaşımında yatmaktadır.*

Results (Bulgular): *It was observed that the experimentally calculated sigma vectors were formed to bring the unnormalized coma vector close to zero, and the calculated misalignments correspond to a CFPP misalignment condition./ Deneysel olarak hesaplanan sigma vektörlerinin, normalleştirilmemiş koma vektörünü sıfıra yaklaştırdığı ve hesaplanan hizalama kaçıklıklarının CFPP hizalama kaçıklığı koşuluyla uyuştuğu gözlemlendi.*

Conclusion (Sonuç): *The CFPP misalignment was successfully established for the Cassegrain telescope, and an aberration analysis was conducted for this specific condition./ Cassegrain teleskobu için CFPP hizalama kaçıklığı başarıyla oluşturulmuş ve bu özel durum için aberasyon analizi gerçekleştirilmiştir.*

*Corresponding author, e-mail: bora@gazi.edu.tr
DOI: 10.29109/gujsc.1586470

GU J Sci, Part C, 12(4): 1145-1154 (2024)

Gazi Üniversitesi
Fen Bilimleri Dergisi
PART C: TASARIM VE TEKNOLOJİ

Gazi University
Journal of Science
PART C: DESIGN AND TECHNOLOGY

http://dergipark.gov.tr/gujsc

Experimental Investigations of Sigma Vectors in Nodal Aberration Theory for Coma-Free Pivot Misalignment State of a Cassegrain Telescope

Meltem YEŞİLTEPE[1], Sefer Bora LİŞESİVDİN[2*]

[1]*Gazi University, Department of Advanced Technologies, 06560, Ankara, Türkiye*

[2]*Gazi University, Department of Physics, 06560, Ankara, Türkiye*

Article Info

Research article
Received: 18/11/2024
Revision: 02/12/2024
Accepted: 03/12/2024

Keywords

Nodal aberration theory
Coma-free pivot point (CFPP)
Cassegrain telescope
Sigma vectors
Optical alignment

Abstract

The study aims to experimentally investigate the sigma vectors in Nodal Aberration Theory for a customized non-aplanatic high-precision Cassegrain telescope, which corrects third-order spherical aberration but not for third-order coma aberration, under coma-free pivot point (CFPP) misalignment conditions. Rotating the telescope's secondary mirror at the CFPP introduces a specific misalignment condition, resulting in unchanged coma aberration across the field of view (FOV). Evaluating CFPP misalignment is essential for optical alignment processes. Investigating the field aberration vectors for the telescope's CFPP misalignment state provides valuable insights into the behavior of field-dependent aberrations and enhances the understanding of CFPP misalignment conditions.

Cassegrain teleskobunun koma-serbest dönme noktası hizalama kaçıklığı durumu için Nodal Aberasyon Teorisi'ndeki sigma vektörlerin deneysel incelenmesi

Makale Bilgisi

Araştırma makalesi
Başvuru: 18/11/2024
Düzeltme: 02/12/2024
Kabul: 03/12/2024

Anahtar Kelimeler

Nodal aberasyon teorisi
Koma-serbest dönme noktası (CFPP)
Cassegrain teleskop
Sigma vektörleri
Optik hizalama

Öz

Bu çalışma, üçüncü derece küresel aberasyonu düzeltebilen ancak üçüncü mertebe koma sapmasını düzeltemeyen, özel olarak tasarlanmış ve yüksek hassasiyetli bir Cassegrain teleskop için Nodal Aberasyon Teorisi'ndeki sigma vektörlerini deneysel olarak incelemeyi amaçlamaktadır. Teleskobun ikincil aynasının koma-serbest dönme noktası (CFPP) üzerinde döndürülmesi, görüş alanı (FOV) boyunca değişmeyen koma aberasyonuna neden olan belirli bir hizalama kaçıklığı durumunu ortaya çıkarır. KSDN hizalama kaçıklıklarını değerlendirmek, optik hizalama süreçleri açısından kritik öneme sahiptir. Teleskobun KSDN hizalama kaçıklığı durumunda alan aberasyon vektörlerinin incelenmesi, alan bağımlı sapmaların davranışına dair önemli bilgiler sağlar ve KSDN hizalama hatası koşullarının daha iyi anlaşılmasını sağlar.

1. INTRODUCTION (GİRİŞ)

Nodal Aberration Theory (NAT) specifies the aberrational behavior of optical systems with misaligned optical components. The theory was initially developed by R. V. Shack, building on the findings of R. A. Buchroeder, who presented the concept of the shifted aberration field centers on the image plane for misaligned optical systems, and H. H. Hopkins, who established conventional aberration theory for rotationally symmetric optical systems [1-3]. K. Thompson further developed the mathematical foundation of NAT, extending it to fifth-order aberrations [4-7]. Thompson also proposed a real-ray-based calculation method for sigma vector contributions, offering an alternative to Buchroeder's approach [8]. T. Schmidt investigated the effect of primary mirror figure

*Corresponding author, e-mail: bora@gazi.edu.tr
DOI: 10.29109/gujsc.1586470

error, which also causes two astigmatism nodes that are symmetrical respecting the center of the image plane in the aligned state [9]. NAT was later expanded by K. Fuerschbach *et al*. to define the aberration characteristics of freeform optical systems, demonstrating the powerful impact of NAT. Due to these contributions, NAT is now a comprehensive theory used for optical design, tolerancing, and alignment processes [10]. However, experimental investigations of NAT are still ongoing [11-13]. In our previous work, sigma vector contributions were calculated using experimental data, and the sigma vectors calculated by the real-ray-based method in design were compared [14]. This study investigates CFPP misalignment, a special case that complicates the optical alignment process in a customized Cassegrain telescope. As is well known, a non-zero on-axis coma measurement for any telescope is an obvious indication of misalignment in optical components [9]. However, an alignment strategy focused solely on removing coma terms from the center of the image plane may not ensure proper telescope alignment. The CFPP can be defined as the point on the primary mirror axis where rotating the secondary mirror does not introduce coma aberration. The location of the CFPP point depends on the structural parameters of the telescope and leads to a specific misalignment condition.

This study presents experimental results for an intentionally misaligned Cassegrain telescope and experimentally calculated sigma vector contributions for the same telescope in a CFPP misalignment state. Section 2 summarizes the theoretical background of Nodal Aberration Theory (NAT) for third-order astigmatism and coma aberrations. Section 3 provides optical specifications and an aberration analysis for the Cassegrain telescope. In Section 4, interferometric measurement results for the misaligned telescope are presented, followed by an analysis of the field aberration vectors and the sigma vectors arising from these misalignments. This study demonstrates an application of NAT that can be used for aligning high-precision, misaligned two-mirror telescope systems.

2. THEORETICAL BACKGROUND (TEORİK ALTYAPI)

As H. H. Hopkins stated, in an optical system with rotational symmetric optical elements, the total third-order aberration amount in the image plane is the sum of the contributions from the surface aberrations. These surface aberrations are rotationally symmetric about the optical axis which serves as the center of the image plane in properly aligned optical system [1,4]. However, when the optical elements are misaligned in a nominally rotationally symmetric system, the center of symmetry for the aberrations of the misaligned surfaces shifts by a certain amount in the image plane, referred to as the sigma vector, and denoted by $\boldsymbol{\sigma}_j$ for surface j. Even in this case, the total amount of third-order aberrations in the image plane remains unchanged. However, incorporating the induced sigma vector for the misaligned components to the nominal field vector of the system alters the field behavior of the third-order aberrations that have field dependence. This change introduces a nodal property (where aberration goes to zero) in the image plane, particularly for third-order astigmatism (W_{222}) and coma (W_{131}) aberrations [4]. This change in the field dependency for misaligned surfaces is given below.

$$\boldsymbol{H}_{Aj} = \boldsymbol{H} - \boldsymbol{\sigma}_j \tag{1}$$

In Eq. (1), $\boldsymbol{H}_{Aj}$ is the effective field vector, $\boldsymbol{H}$ is the field vector for a nominal optical system, and $\boldsymbol{\sigma}_j$ is the sigma vector for the misaligned surface j. In this study, vector quantities are represented in bold. A graphical representation of these vectors is illustrated in Figure 1.

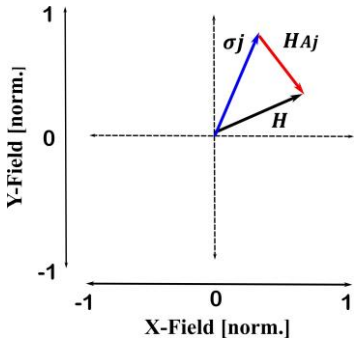

Figure 1. Representation of effective field vector $\boldsymbol{H}_{Aj}$, field vector $\boldsymbol{H}$, and sigma vector $\boldsymbol{\sigma}_j$ (Etkin alan vektörünün $\boldsymbol{H}_{Aj}$, alan vektörünün $\boldsymbol{H}$, ve sigma vektörün $\boldsymbol{\sigma}_j$ gösterimi)

Note that, the sigma vector for an aspherical surface consists of two components: the spherical and the aspherical. The spherical contribution, denoted by $\boldsymbol{\sigma}_j^{sph}$ for surface j, arises due to the spherical base curve and indicates the new symmetry center of the spherical aberration contributions of surface j. The aspherical contribution, denoted by $\boldsymbol{\sigma}_j^{asph}$ for surface j, originates from deviations from a spherical base curve and signifies the aberration symmetry center of the aspherical surface aberration contributions of the subjected surface [4,

8]. In the following sections, the notations "*sph*" and "*asph*" will be employed to distinguish between the spherical and aspherical contributions. It is important to calculate these two vector contributions independently.

Third-order coma aberration expression for a misaligned telescope can be expressed as

$$W = [(W_{131}\boldsymbol{H} - \boldsymbol{A}_{131}).\boldsymbol{\rho}].\boldsymbol{\rho}^{\boldsymbol{2}} \quad (2)$$

where W_{131} is the system-level third-order coma aberration obtained by summating the coma contributions from the individual optical components and $\boldsymbol{\rho}$ is the normalized aperture vector. $\boldsymbol{A}_{131}$ is an unnormalized displacement vector resulting from the aggregation of the sigma vectors of the individual surfaces weighted by their corresponding surface aberration contributions for coma. $\boldsymbol{A}_{131}$ is expresses as

$$\boldsymbol{A_{131}} = \sum (W_{131,j}^{sph}\,\boldsymbol{\sigma}_j{}^{sph} + W_{131,j}^{asph}\boldsymbol{\sigma}_j{}^{asph}) \quad (3)$$

In Eq. (3), $W_{131,j}{}^{sph}$ and $W_{131,j}{}^{asph}$ represent spherical and aspherical contributions of third-order coma for surface *j*, respectively. To compute the coma node location, the expression given in the square bracket in Eq. (2) is set to zero, and the equation is solved for $\boldsymbol{H}$. The coma node location ($\boldsymbol{a}_{131}$) is given as

$$\boldsymbol{a}_{131} = \frac{\boldsymbol{A}_{131}}{W_{131}} \quad (4)$$

As indicated in Eq. (4), misalignments of the optical components cause the coma node to shift to a different point in the image plane, resulting in non-zero measurements of third-order coma-related Fringe Zernike Coefficients (FZC) at the center of the image plane. However, there is an exception for the CFPP misalignment which is a state where the axial misalignment of M2 is compensated by tilt. Even if the third-order coma-related terms are absent at the center of the image plane, the optical system may still be misaligned (Figure 2(a)).

For a two-mirror telescope, if the primary mirror (M1) is used as an aperture stop and the secondary mirror (M2) is misaligned, $\boldsymbol{A}_{131} = 0$ condition is satisfied for $\boldsymbol{\sigma}_{M2}{}^{sph} \neq 0$ and $\boldsymbol{\sigma}_{M2}{}^{asph} \neq 0$. The equation is provided below [16].

$$\boldsymbol{A}_{131} = \left(W_{131,M2}{}^{sph}\,\boldsymbol{\sigma}_{M2}{}^{sph} + W_{131,M2}{}^{asph}\boldsymbol{\sigma}_{M2}{}^{asph}\right) = 0 \quad (5)$$

Utilizing the Eq. (5), the following expression can be derived.

$$\frac{\boldsymbol{\sigma}_{M2,(x,y)}{}^{sph}}{\boldsymbol{\sigma}_{M2,(x,y)}{}^{asph}} = -\frac{W_{131,M2}{}^{asph}}{W_{131,M2}{}^{sph}} \quad (6)$$

The expression given above can be achieved by infinite combination of $\boldsymbol{\sigma}_{M2}{}^{sph}$ ve $\boldsymbol{\sigma}_{M2}{}^{asph}$. An example illustrating the third-order coma and astigmatism aberrations for the CFPP state of a non-aplanatic Cassegrain telescope is provided in Figure 2. To align such a telescope system, both third-order coma and astigmatism aberrations in the image plane must be considered.

The location of the CFPP depends on the structural parameters of the telescope and is shown in Figure 2(c) [16]. In Figure 2(c), $L_{M2}^{(CFPP)}$ is a general representation of the location of the CFPP for a two mirror telescope. $L_{M2}^{(CFPP)}$ is measured from the nominal vertex of the M2. Specifically, for a Cassegrain telescope where the primary mirror serves as the aperture stop, $L_{M2}^{(CFPP)}$ and the prime focus coincide with each other.

Third-order astigmatism aberration expression for a misaligned telescope can be expressed as [4]

$$W = \frac{1}{2}\left[W_{222}\boldsymbol{H}^{\boldsymbol{2}} - 2\boldsymbol{H}\boldsymbol{A_{222}} + \boldsymbol{B}_{\boldsymbol{222}}^{\boldsymbol{2}}\right].\rho^2 \quad (7)$$

where the W_{222} is the overall third-order astigmatism aberration is obtained by summing the astigmatism contributions of the individual optical components. $\boldsymbol{A_{222}}$ is the unnormalized vector resulting from the aggregation of the sigma vectors of the individual surfaces weighted by their respective surface aberration contributions for astigmatism. $\boldsymbol{A_{222}}$ can be expresses as

$$\boldsymbol{A}_{222} = \sum_j \left(W_{222,j}{}^{sph}\boldsymbol{\sigma}_j{}^{sph} + W_{222,j}{}^{asph}\boldsymbol{\sigma}_j{}^{asph}\right) \quad (8)$$

$\boldsymbol{B_{222}^2}$ is un-normalized squared vector resulting from the aggregation of squares of sigma vectors weighted by corresponding surface aberration contributions for astigmatism, respectively. $\boldsymbol{B_{222}^2}$ can be written as

$$\boldsymbol{B}_{222}^2 = \sum_j \left(W_{222,j}{}^{sph}\boldsymbol{\sigma}_j{}^{sph^2} + W_{222,j}{}^{asph}\boldsymbol{\sigma}_j{}^{asph^2}\right) \quad (9)$$

If the overall third-order astigmatism is not zero, two astigmatism nodes arise when the optical system is misaligned. To determine the astigmatism node locations, the expression given in the square bracket is set to zero, and the resulting quadratic equation is solved for $\boldsymbol{H}$. The node locations are then computed as

$$\boldsymbol{H} = \frac{\boldsymbol{A}_{222} \pm i\sqrt{W_{222}\boldsymbol{B}_{222}^2 - \boldsymbol{A}_{222}^2}}{W_{222}} \tag{10}$$

By normalizing $\boldsymbol{A_{222}}$ and $\boldsymbol{B_{222}^2}$ vectors by overall astigmatism, the $\boldsymbol{a_{222}}$ and $\boldsymbol{b_{222}^2}$ vector pair are yielded as

$$\boldsymbol{a}_{222} \equiv \frac{\boldsymbol{A}_{222}}{W_{222}} \tag{11}$$

$$\boldsymbol{b_{222}^2} \equiv \frac{\boldsymbol{B}_{222}^2}{W_{222}} - \boldsymbol{a_{222}^2} \tag{12}$$

where $\boldsymbol{a_{222}}$ and $\boldsymbol{b_{222}}^{\boldsymbol{2}}$ are normalized vectors in the image plane. The node positions rewritten with normalized vectors is as

$$\boldsymbol{H} = \boldsymbol{a}_{222} \pm i\boldsymbol{b}_{222}^2 \tag{13}$$

To calculate astigmatism node locations analytically, we square both sides of the equation as described below.

$$0 = (\boldsymbol{H} - \boldsymbol{a}_{222})^2 + \boldsymbol{b}_{222}^2 \tag{14}$$

The studies provide an extensive detailed calculation of the astigmatism node locations and nodal aberration [4, 16].

The expressions of the sigma vector contributions in terms of the structural parameters of the telescope with secondary mirror misalignments (M1 is aperture stop) are also given below [16].

$$\boldsymbol{\sigma}_{M2,x}{}^{sph} = -\frac{XDE_{M2} - BDE_{M2}r_{M2}}{\bar{u}_{M1}(d_1 + r_{M2})} \tag{15}$$

$$\boldsymbol{\sigma}_{M2,y}{}^{sph} = -\frac{YDE_{M2} + ADE_{M2}r_{M2}}{\bar{u}_{M1}(d_1 + r_{M2})} \tag{16}$$

$$\boldsymbol{\sigma}_{M2,x}{}^{asph} = -\frac{XDE_{M2}}{d_1\bar{u}_{M1}} \tag{17}$$

$$\boldsymbol{\sigma}_{M2,y}{}^{asph} = -\frac{YDE_{M2}}{d_1\bar{u}_{M1}} \tag{18}$$

where d_1, r_{M2} and $\bar{u}_{M1}$are the distance between M1 and M2 mirrors, the radius of curvature of M2 and the chief ray incidence angle on M1, respectively. Furthermore, XDE_{M2} and YDE_{M2} are defined as the X and Y decenter amounts along the M2 mirror, respectively. Similarly, ADE_{M2} and BDE_{M2} are defined as the X and Y tilt amounts about the X and Y-axis, respectively.

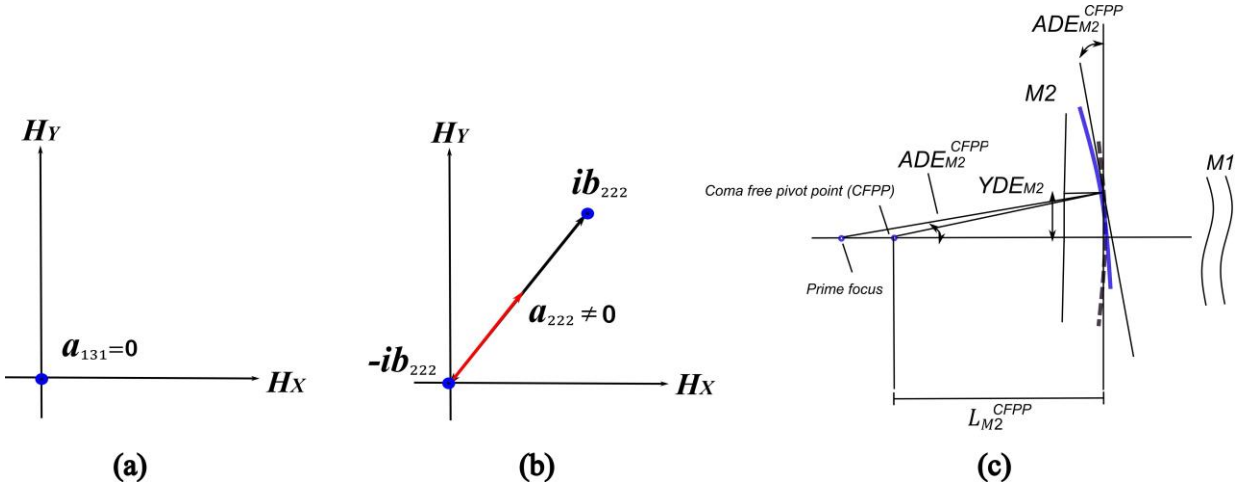

Figure 2. a) Third-order coma node location, b) astigmatism node locations (for CFPP misalignment), c) CFPP location of the M2 (a)Üçüncü derece koma b) astigmatizm nod lokasyonları, c) M2 için KSDN noktasının lokasyonu)

2. CASSEGRAIN TELESCOPE DESIGN (CASSEGRAIN TELESKOP TASARIMI)

The high-precision two-mirror telescope was designed in the Cassegrain configuration, featuring a concave parabolic primary mirror and a convex hyperbolic secondary mirror that eliminates the third-order spherical aberration [17]. The radii of curvature for the primary and secondary mirrors are -1700 mm and -300 mm, respectively. Additionally,

the conic constant of the secondary mirror is -1.737. The signs of these structural parameters are determined by the sign convention used for the mirrors. The technical specifications (Table 1) and schematic design layout of the Cassegrain telescope are provided in Figure 3.

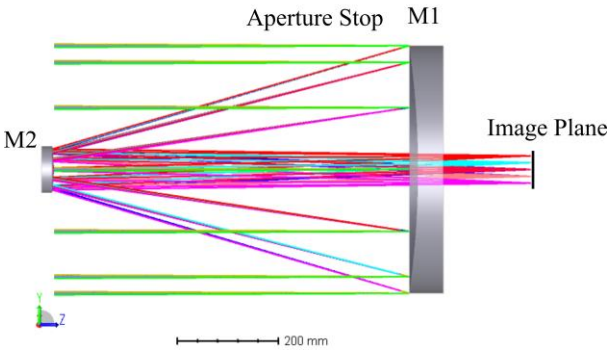

Figure 3. Optical design layout of the Cassegrain telescope (Cassegrain teleskop optik tasarım çizimi)

Table 1. Technical Specifications for the F/12.7 Cassegrain telescope (F/12.7 Cassegrain teleskop için teknik spesifikasyonlar)

Parameter	**Unit**	**Value**
Entrance Pupil Diameter (EPD)	mm	490
Wavelength (λ)	nm	633
Effective Focal Length (EFFL)	mm	6200
Linear Obscuration (γ)	%	20
Overall Length (L)	mm	944

Paraxial ray-tracing data obtained from the optic design software, in Table 2, was utilized to calculate the third-order spherical aberration, coma, and astigmatism aberration surface contributions. In Table 2, y and $\bar{y}$ are marginal and chief ray heights at surface, respectively. Similarly, u and $\bar{u}$ are marginal and chief ray angles at surfaces, respectively. EP refers to the entrance pupil. Calculation results for the aberration coefficients are provided in Table 3. Graphical representations for the surface aberration contributions are also given in Figure 4. In Table 3, ${W_{040,M1/M2}}^{sph}$ and ${W_{040,M1/M2}}^{asph}$ are spherical and aspherical spherical aberration contributions, respectively.

As shown clearly in Figure 4(a), the third-order spherical aberration is corrected by design. Due to its parabolic shape, the primary mirror can eliminate third-order spherical aberration by integrating its spherical and aspherical spherical aberration contributions. The secondary mirror can also correct the third-order spherical aberration introduced by its shape. The residual third-order spherical aberration in the image plane results from limitations in manufacturing precision. In Figure 4(b) and Figure 4(c), since the Cassegrain telescope cannot correct third-order coma and astigmatism aberrations, residual coma ($W_{131} \neq 0$) and astigmatism ($W_{222} \neq 0$) are visible in the focal plane. The Cassegrain telescope inherently has the third-order coma, which has a linear field dependency, and astigmatism, which has quadratic field dependency, aberrations at the system level, which are distributed along the FOV according to their respective field dependencies. The Full Field Displays (FFDs) for the Cassegrain telescope in design are illustrated in Figure 5. In Figure 5(a), the magnitude of the third-order coma-related FZCs (Z_7 and Z_8) are given and in Figure 5(b), the magnitude of the third-order astigmatism-related FZCs (Z_5 and Z_6) are presented. The equations for calculation of the $Z_{7/8}$ and $Z_{5/6}$ are provided below.

$$Z_{7/8} = \sqrt{Z_7^2 + Z_8^2} \tag{19}$$

$$Z_{5/6} = \sqrt{Z_5^2 + Z_6^2} \tag{20}$$

As stated in the previous section, to create a misalignment condition resulting in the CFPP concept, the $\boldsymbol{A}_{131}$ vector needs to be zero for ${\boldsymbol{\sigma}_{M2}}^{sph} \neq 0$ and ${\boldsymbol{\sigma}_{M2}}^{asph} \neq 0$. The ratio given in Eq. (6) is 0.931 for the Cassegrain telescope configuration as shown in Eq. (21).

$$\frac{{\boldsymbol{\sigma}_{M2,(x,y)}}^{sph}}{{\boldsymbol{\sigma}_{M2,(x,y)}}^{asph}} = -\frac{{W_{131,M2}}^{asph}}{{W_{131,M2}}^{sph}} = 0.931 \tag{21}$$

Table 2. Paraxial Ray-Tracing Data from OpticStudio optical design software (Optik tasarım programından elde edilen paraksiyal ışın izleme verileri)

Surface#	$\boldsymbol{y}$ $(\boldsymbol{mm})$	$\boldsymbol{u}$ $(\boldsymbol{deg.})$	$\bar{\boldsymbol{y}}$ $(\boldsymbol{mm})$	$\bar{\boldsymbol{u}}$ $(\boldsymbol{deg.})$	**Description**
OBJ	0	0	Infinity	0.00436	OBJ.
1	245.00000	0	-3.70885	0.00436	EP
STOP	245.00000	0.28824	0	-0.00436	M1 Mirror/STOP
3	37.30436	-0.03952	3.14412	0.02533	M2 Mirror

IMG	0.00635	-0.03952	27.04925	0.02533	IMG.

Table 3. Third-order spherical aberration, coma and astigmatism surface aberration contributions ($\lambda = 632.8$ nm) (Üçüncü derece küresel aberasyon, koma ve astigmatizm yüzey aberasyon katkıları)

Surface #	$W_{040}^{sph}(\lambda)$	$W_{040}^{asph}(\lambda)$	$W_{131}^{sph}(\lambda)$	$W_{131}^{asph}(\lambda)$	$W_{222}^{sph}(\lambda)$	$W_{222}^{asph}(\lambda)$
M1	289.731	-289.731	-35.088	0	1.062	0
M2	-49.220	49.236	17.835	16.599	-1.616	1.399
Total	240.510	-240.495	-17.253	16.599	-0.553	1.399
	0.0153		-0.6543		0.8458	

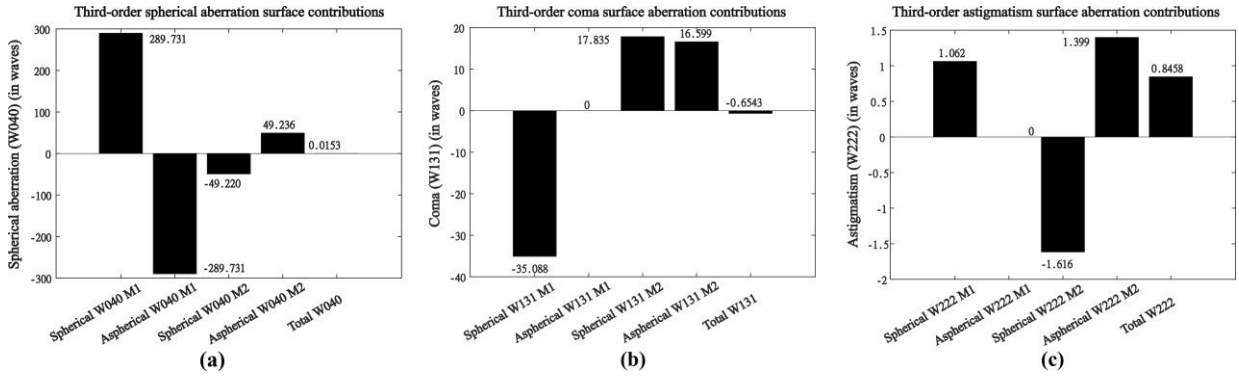

Figure 4. a) Third-order spherical aberration, b)coma, and c) astigmatism contributions (a) Üçüncü dereceden küresel aberasyon, b) koma ve c) astigmatizm katkıları)

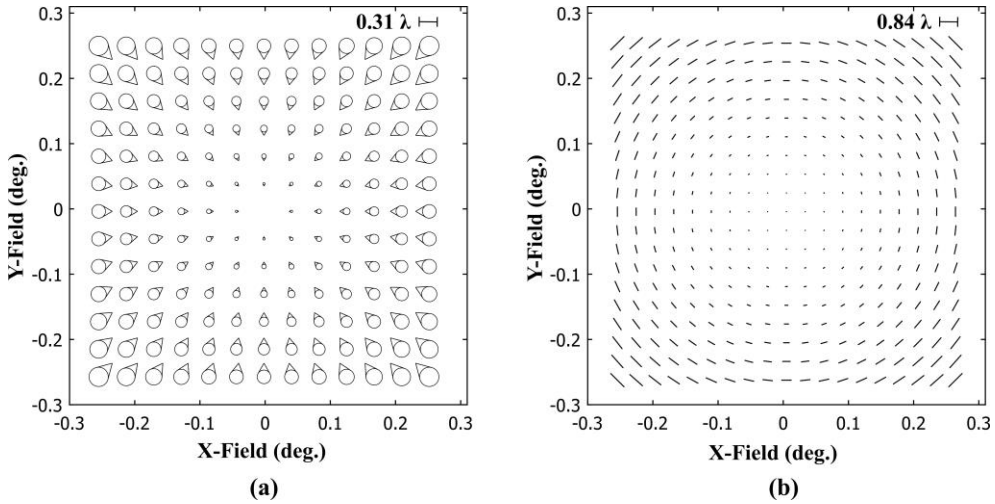

Figure 5. Full Field Displays for (a) Third-order coma, and (b) third-order astigmatism aberration (a) Üçüncü dereceden koma ve (b) üçüncü dereceden astigmatizma aberasyonları için Tüm Alan Gösterimleri)

3. EXPERIMENTAL INVESTIGATION (DENEYSEL İNCELEME)

3.1. Experimental setup (Deney düzeneği)

The test configuration includes a Fizeau phase-shifting interferometer (with a transmission sphere) mounted on a five-axis stage, a telescope, piezo actuators that enable movement of the telescope's secondary mirror, and a flat mirror with its control unit. In this configuration, the focal point of the interferometer's transmission element is aligned to coincide with the telescope's focal plane. 632.8 nm wavelength laser beam enters the telescope at the focal plane, reflects of the M2 and M1 mirror surfaces, and reaches the reference mirror. The beam then follows the reverse optical path back to

the interferometer, which analyzes the difference between the reference and reflected beams. By scanning the entire image plane, the aberration state of the telescope can be observed. In this study, nine field points arranged in a 3×3 matrix in the image plane were selected for calculating the sigma vector contributions to simplify the data-gathering process.

The X and Y field angle coordinates of the selected field points from the image plane (where the field point (0°, 0°) refers to the center of the image plane), used for the calculation, are provided in Table 4. The schematic diagram of the experimental setup is illustrated in Figure 6.

Table 4. Selected field points in the Cassegrain telescope image plane (Cassegrain teleskopun görüntü düzleminde seçilen alan noktaları)

-0.125°, 0.125°	0°, 0.125°	0.125°, 0.125°
(-0.125°, 0°)	(0°, 0°)	0.125°, 0°
-0.125°, -0.125°	0°, -0.125°	0.125°, -0.125°

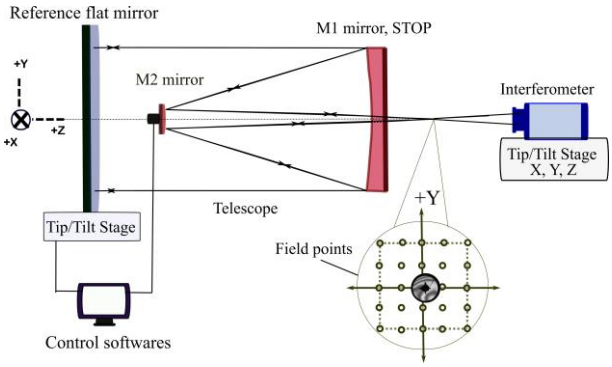

Figure 6. Experimental set-up for interferometric measurements (Interferometrik ölçümler için deney düzeneği)

3.2. Calculation of sigma vectors for CFPP misalignment (CFPP hizalama kaçıklığı durumu için sigma vektörlerinin hesaplanması)

The secondary mirror of the telescope was intentionally misaligned to create a misalignment condition where the distribution of third-order coma aberration terms remains uniform across the field of view similar to the aligned state, while the astigmatism aberration terms become asymmetrical, resulting in a binodal astigmatism in the image plane. Raw interferometric measurements were taken from the image plane, as illustrated in Figure 7.

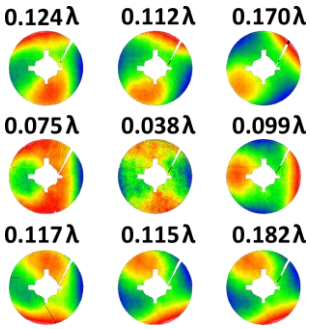

Figure 7. Interferometric RMS WFE measurements taken from the focal plane (3x3 field points) (Odak düzleminden alınan interferometrik RMS WFE ölçümleri (3x3 alan noktası)

The raw interferometric measurements include third-order spherical aberration, third-order coma and astigmatism-related FZCs and which can be isolated from the raw measurement data. The FZCs, Z_5(Astigmatism 0°/90°), Z_6 (Astigmatism ±45°), Z_7(X-Coma), Z_8 (Y-Coma), were isolated from the measured raw data. The interferograms for the magnitudes of the third-order astigmatism ($Z_{5/6}$) and coma ($Z_{7/8}$) related terms are illustrated Figure 8.

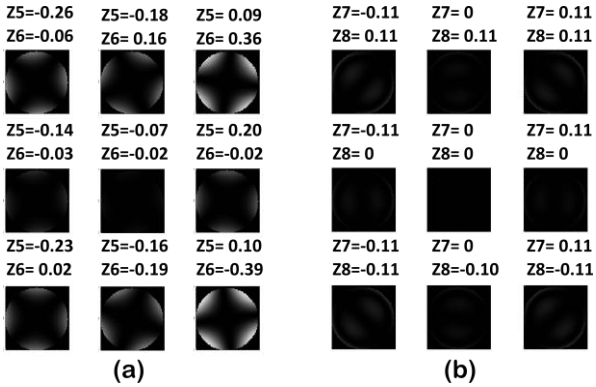

Figure 8. Magnitudes of a) astigmatism and, b) coma FZCs (a) astigmatizm ve b) koma FZC terimlerinin büyüklükleri)

As seen in Figure 8(a), the astigmatism aberration distribution along the full FOV appears to be non-rotationally symmetric which is clear sign of the misalignment. In this case, the third-order astigmatism shows unique binodal behavior as predicted by NAT. Note that in Figure 8(a), the primary mirror figure error was not removed from the data. Note that in Figure 8(a), the primary mirror figure error was not removed from the data. The effect of the primary mirror figure error was examined experimentally in our previous research paper [15]. In Figure 8(b), the coma aberration distribution along the FOV appears to be rotationally symmetric. This special misalignment

case can serve as an example case for a CFPP misalignment of a Cassegrain telescope. Each third-order coma-related FZC term obtained from the on-axis point was measured to be around 0.003λ, which is considered negligible and attributed to environmental instabilities in the experimental conditions, such as turbulence. By fitting the measured astigmatism and coma FZCs to the relevant polynomials, the locations of the field aberration vectors were experimentally calculated and are presented in Table 5.

Table 5. Calculated field aberration vectors
(Hesaplanan alan aberasyon vektörleri)

Field aberration vectors	X-component	Y-component
$\boldsymbol{a}_{222}$	-0.41286	-0.00893
$\boldsymbol{a}_{131}$	0.00966	-0.01150

The sigma vector contributions of the telescope's secondary mirror are calculated as given in **Hata! B aşvuru kaynağı bulunamadı.**.

Table 6. Calculated sigma vectors (Hesaplanan sigma vektörler)

Sigma vectors of M2	X-component	Y-component
$\boldsymbol{\sigma}_{M2}{}^{sph}$	0.11179	0.00263
$\boldsymbol{\sigma}_{M2}{}^{asph}$	-0.12051	-0.00237

For the $\boldsymbol{A}_{131} = 0$ condition, For the $\boldsymbol{A}_{131} = 0$ condition, the ratio given in Eq. (21) was calculated using the sigma vector contributions shown in **Hata! Başvuru kaynağı bulunamadı.**.

$$\frac{\boldsymbol{\sigma}_{M2,x}{}^{sph}}{\boldsymbol{\sigma}_{M2,x}{}^{asph}} = -\frac{0.11179}{(-0.12051)} = -0.928 \quad (22)$$

$$\frac{\boldsymbol{\sigma}_{M2,y}{}^{sph}}{\boldsymbol{\sigma}_{M2,y}{}^{asph}} = -\frac{0.00263}{(-0.00237)} = -1.110 \quad (23)$$

By combining the calculated $\boldsymbol{\sigma}_{M2}{}^{sph}$ vectors with the structural parameters of the telescope, misalignment amounts can be easily determined using Eq. (15), Eq. (16), Eq. (17), and Eq. (18), as given in Table 7.

The graphical representation of the sigma vectors is illustrated in Figure 9(a). Furthermore, calculated misalignments were simulated in the optical design software and the nodes induced by the misalignments are demonstrated in Figure 9(b) and Figure 9(c).

Table 7. Calculated misalignment amounts for the secondary mirror of Cassegrain telescope (Cassegrain teleskopun ikinci aynası için hesaplanan hizalama kaçıklıkları miktarları)

Misalignments	$\boldsymbol{XDE}_{\boldsymbol{M2}}$ (mm)	$\boldsymbol{YDE}_{\boldsymbol{M2}}$ (mm)	$\boldsymbol{ADE}_{\boldsymbol{M2}}$ (deg.)	$\boldsymbol{BDE}_{\boldsymbol{M2}}$ (deg.)
Value	-0.3788	-0.0074	0.0036	-0.1674

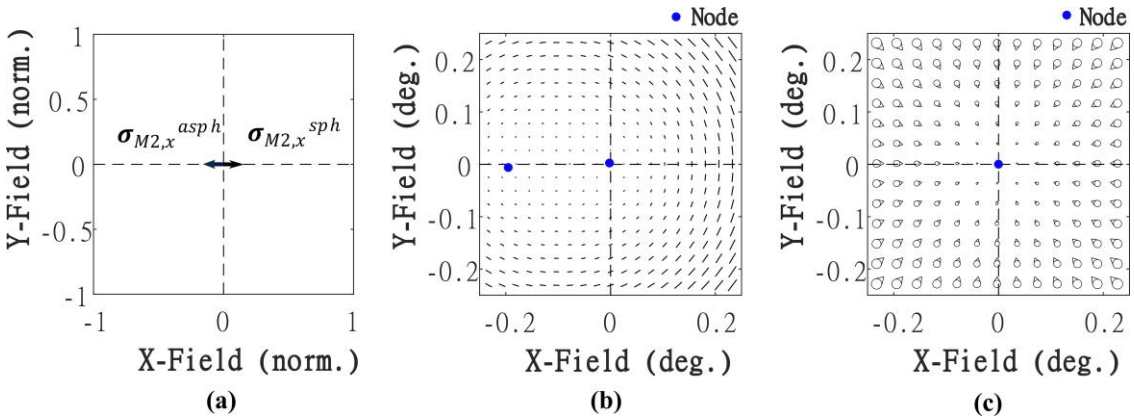

Figure 9. (a) Sigma vector components of M2, (b) graphical illustration of the astigmatism aberration free and (c) coma aberration free points (a) M2'nin sigma vektör bileşenleri, (b) astigmatizm ve c) koma aberasyonlarının sıfır olduğu noktaların (nod) grafiksel gösterimi)

2. CONCLUSIONS (SONUÇLAR)

The calculation of field aberration vectors and sigma vectors for a Cassegrain telescope operating in a CFPP misalignment state has been experimentally investigated in this study. A controlled misalignment state was obtained using compensatory misalignments to remove on-axis coma terms by purposefully rotating the

secondary mirror. The experimental results confirm that the CFPP configuration produces a specific aberration distribution, with the third-order coma node located at the on-axis point. This configuration allows the alignment process to be simplified, requiring only the determination of the astigmatism field aberration vector location. This work contributes to the field of telescope alignment and aberration management by demonstrating how the predictable coma-free behavior and binodal property of astigmatism can streamline the alignment process. This leads to more precise calculations of misalignments and a reduction in the number of alignment steps. It establishes the foundation for future studies of complex misalignment states in other optical systems by providing a valuable framework for investigating sigma vector behavior under CFPP settings. To improve their suitability for in sophisticated optical systems, future research may concentrate on improving existing techniques and investigating novel aberration contributions.

ACKNOWLEDGMENTS (TEŞEKKÜR)

The authors would like to thank Dr. Özgür Karcı and Mustafa Ekinci for their support and for the resources they made available. The authors would also like to thank Eray Arpa for his valuable assistance.

DECLARATION OF ETHICAL STANDARDS (ETİK STANDARTLARIN BEYANI)

The author of this article declares that the materials and methods they use in their work do not require ethical committee approval and/or legal-specific permission.

Bu makalenin yazarı çalışmalarında kullandıkları materyal ve yöntemlerin etik kurul izni ve/veya yasal-özel bir izin gerektirmediğini beyan ederler.

AUTHORS' CONTRIBUTIONS (YAZARLARIN KATKILARI)

***Meltem YEŞİLTEPE*:** She conducted the experiments, analyzed the results and performed the writing process.

Deneyleri yapmış, sonuçlarını analiz etmiş ve maklenin yazım işlemini gerçekleştirmiştir.

Sefer Bora LİŞESİVDİN: He analyzed the results and performed the writing process.

Sonuçlarını analiz etmiş ve maklenin yazım işlemini gerçekleştirmiştir.

CONFLICT OF INTEREST (ÇIKAR ÇATIŞMASI)

There is no conflict of interest in this study.

Bu çalışmada herhangi bir çıkar çatışması yoktur.

REFERENCES (KAYNAKLAR)

[1] Hopkins H. H., (1950), Wave Theory of Aberrations, Clarendon Press.

[2] Buchroeder R. A., (1976), Tilted Component Optical Systems, Ph.D. Thesis, The University of Arizona, Tucson.

[3] Shack R. V., and Thompson K., Influence of alignment errors of a telescope system on its aberration field, 251 (1980) 146-53.

[4] Thompson K. P., Description of the third-order optical aberrations of near-circular pupil optical systems without symmetry, Journal of the Optical Society of America A, 22 (2005) 1389-401.

[5] Thompson K. P., 'Multinodal fifth-order optical aberrations of optical systems without rotational symmetry: spherical aberration', Journal of the Optical Society of America A, 26, (2009) 1090-100.

[6] Thompson K. P., 'Multinodal fifth-order optical aberrations of optical systems without rotational symmetry: the comatic aberrations', Journal of the Optical Society of America A, 27, (2010), 1490-504.

[7] Thompson K. P., Multinodal fifth-order optical aberrations of optical systems without rotational symmetry: the astigmatic aberrations', Journal of the Optical Society of America A, 28 (2011) 821-36.

[8] Thompson K. P., Schmid T., Cakmakci O., and Rolland J. P., Real-ray-based method for locating individual surface aberration field centers in imaging optical systems without rotational symmetry, Journal of the Optical Society of America A, 26 (2009) 1503-17.

[9] Schmid, T., Rolland J. P., Rakich A., and Thompson K. P., Separation of the effects of astigmatic figure error from misalignments using Nodal Aberration Theory (NAT), Optics Express, 18 . (2010) 17433-47.

[10] Fuerschbach, K., Rolland J. P., and Thompson K. P. Theory of aberration fields for general optical systems with freeform surfaces, Optics Express, 22 (2014) 26585-606.

[11] Zhao N., Papa J. P., Fuerschbach K., Qiao Y., Thompson K. P., and Rolland J. P., Experimental investigation in nodal aberration theory (NAT) with a customized Ritchey-Chrétien system: third-order coma, Optics Express, 26 (2018) 8729-43.

[12] Karcı Ö., Arpa E., Ekinci M., and Rolland J. P., 2021. Experimental investigation of binodal astigmatism in nodal aberration theory (NAT) with a Cassegrain telescope system, Optics Express, 29 (2021) 19427-40.

[13] Karcı Ö., A simulation and experimental validation of third-order coma in nodal aberration theory with a Cassegrain telescope', Turkish Journal of Physics, 45 (2021) 378-89.

[14] Karcı, Ö., Yeşiltepe M., Arpa E., Wu Y., Ekinci M., and Rolland J. P., Experimental investigation in nodal aberration theory (NAT): separation of astigmatic figure error from misalignments in a Cassegrain telescope', Optics Express, 30, (2022) 11150-64.

[15] Yeşiltepe M., Bauer A., Karcı Ö., and Rolland J. P., Sigma vector calculations in nodal aberration theory and experimental validation using a Cassegrain telescope, Optics Express, 31 (2023) 42373-87.

[16] Schmid T., (2010). Misalignment induced nodal aberration fields and their use in the alignment of astronomical telescopes, Ph.D. Thesis, University of Central Florida, Orlando.

[17] Karcı Ö., Ekinci M., Design of a high-precision, 0.5 m aperture Cassegrain collimator, Applied Optics, 59 (2020) 8434-42.